

Received: 2017.10.30
Accepted: 2018.01.16
Published: 2018.02.11

Ursolic Acid Attenuates High Glucose-Mediated Mesangial Cell Injury by Inhibiting the Phosphatidylinositol 3-Kinase/Akt/Mammalian Target of Rapamycin (PI3K/Akt/mTOR) Signaling Pathway

Authors' Contribution:
Study Design A
Data Collection B
Statistical Analysis C
Data Interpretation D
Manuscript Preparation E
Literature Search F
Funds Collection G

ABCDEF **Er-Min Wang**
AG **Qiu-Ling Fan**
BC **Yuan Yue**
CF **Li Xu**

Department of Nephrology, First Hospital of China Medical University, Shenyang, Liaoning, P.R. China

Corresponding Author: Qiu-Ling Fan, e-mail: cmufql@163.com

Source of support: National Natural Science Foundation of China (81770724,81270808); Natural Science Foundation of Liaoning Province (201602821); and the Science and Technology Planning Program of Shenyang City (F16-205-1-40)

Background: To investigate the protective effect of ursolic acid (UA) on high glucose (HG)-induced human glomerular mesangial cell injury and to determine whether UA inhibits cell proliferation and reactive oxygen species (ROS) production by suppressing PI3K/Akt/mTOR pathway activation.

Material/Methods: Human mesangial cells were cultured with normal glucose (NG group), high glucose (HG group), mannitol (mannitol hypertonic control group), or high glucose with different concentrations (0.5, 1.0, and 2.0 mmol/L) of UA (HG+UA groups). Cell proliferation and intracellular ROS levels were assessed by methyl thiazolyl tetrazolium (MTT) and dichloro-dihydro-fluorescein diacetate (DCFH-DA) flow cytometry assays, respectively. Western blotting was used to detect mesangial cell expression of PI3K/Akt/mTOR pathway components, including Akt, p-Akt, mTOR, and p-mTOR, and proteins related to cell injury, including TGF- β 1 and fibronectin (FN). mRNA expression of TGF- β 1 and FN were evaluated using real-time quantitative polymerase chain reaction (PCR).

Results: Abnormal proliferation was observed in human glomerular mesangial cells at 48 h after treatment with HG, and UA suppressed the HG-induced proliferation of mesangial cells in a dose-dependent manner. UA inhibited ROS generation and oxidative stress in mesangial cells and mitigated mesangial cell injury. Treatment with UA reduced Akt and mTOR phosphorylation levels in mesangial cells exposed to HG ($p < 0.05$ vs. HG) and downregulated protein and mRNA expression of TGF- β 1 and FN in these cells ($p < 0.05$ vs. HG).

Conclusions: UA attenuated mesangial cell proliferation and ROS generation by inhibiting HG-mediated PI3K/Akt/mTOR pathway activation, thereby ameliorating mesangial cell damage.

MeSH Keywords: **Glucose • Mesangial Cells • Phosphatidylinositol 3-Kinases**

Full-text PDF: <https://www.medscimonit.com/abstract/index/idArt/907814>

 2529

 1

 6

 20



Background

The morbidity of diabetes has increased rapidly in the past decade. Diabetic nephropathy (DN) is a serious complication of diabetes and is the most common cause of end-stage renal disease [1]. A typical pathological feature of DN [2], glomerulosclerosis is primarily manifested as deposition of extracellular matrix (ECM) proteins, such as collagen and fibronectin (FN), in the mesangial area, and the resulting reduced filtration surface area of glomerular capillaries leads to further progression of DN [3]. PI3K/Akt/mTOR signaling is a classical pathway that regulates many cellular functions, such as glucose metabolism, glycogen synthesis, protein synthesis, cell proliferation, cell hypertrophy, and cell death [4], and previous studies have shown that the PI3K/Akt/mTOR pathway is involved in the pathogenesis of DN. High glucose (HG) levels activate phosphatidylinositol-3-kinase (PI3K) in mesangial cells, which stimulates phosphoinositide-dependent kinase (PDK) and protein kinase B (PKB) and subsequently upregulates expression of RhoA, Rac, and type I collagen, inducing an inflammatory response in these cells [5], which leads to damage.

The plant-derived pentacyclic triterpene ursolic acid (UA), which is found widely in berries, fruits, and herbs, exhibits anti-tumor, anti-liver fibrosis, hypoglycemic, hypolipidemic, and anti-atherosclerotic effects [6–11]. Previous studies have found that UA inhibits overexpression of inducible nitric oxide synthase (iNOS) by suppressing STAT-3, ERK1/2, and JNK pathway activation and alleviates glomerular hypertrophy and the increased ECM deposition typically observed in a streptozotocin-induced DN rat model, thus delaying DN progression [12]. However, the detailed mechanism of UA-mediated renal protection remains unclear and requires in-depth analysis.

This study aimed to investigate the effect of UA on the proliferation of human mesangial cells cultured *in vitro* under HG conditions, to determine whether UA has a protective effect on mesangial cell injury under diabetic conditions and to determine whether the mechanism occurs through regulation of the PI3K/Akt/mTOR pathway.

Material and Methods

Materials

Cells and reagents

The following cells, reagents, and antibodies were used in this study: human glomerular mesangial cells (ScienCell Research Laboratories); 4201 standard mesangial cell medium (MCM; ScienCell Research Laboratories); UA (Sigma, US); methyl thiazolyl tetrazolium (MTT) powder (Sigma, US);

dichloro-dihydro-fluorescein diacetate (DCFH-DA) Reactive Oxygen Species (ROS) Detection Kit (Wuhan Beyotime); TRIzol RNA Extraction Kit (Invitrogen, US); GoTaq Quantitative Polymerase Chain Reaction (qPCR) Master Mix (Promega, US); rabbit anti-Akt, anti-p-Akt (p-Ser473), anti-mTOR and anti-p-mTOR (Ser2448) polyclonal antibodies (Cell Signaling Technology, US); rabbit anti-TGF β 1, anti-FN, anti-Bax, anti-Samd2/3, anti-Samd7 and anti-GAPDH polyclonal antibodies (Proteintech, US); and horseradish peroxidase (HRP)-labeled goat anti-rabbit IgG (Abcam, US).

Methods

Mesangial cell culture: Human mesangial cells were thawed and cultured in MCM 4201 at 37°C in an incubator with 5% CO₂ and saturated humidity for cell adherence to the culture dish. The culture medium was changed every other day. The cells were trypsinized with 0.25% trypsin for passaging. Cells in exponential growth phase from the 5th to 9th passages were used for subsequent experiments after they had attached to the culture dish and reached 70–80% confluence.

Groups: Cells were divided into the following groups at 24 h after synchronization in serum-free culture medium: (1) normal glucose (NG) group (5.5 mmol/L glucose); (2) HG group (30.0 mmol/L glucose); (3) UA group (30.0 mmol/L glucose+0.5, 1.0, or 2.0 mmol/L UA); and (4) mannitol hypertonic control group (5.5 mmol/L glucose+24.5 mmol/L mannitol, MA).

Detection of cell proliferation using MTT assays: Cells in exponential growth phase were collected. After adjusting the cell density of the suspension, 150 ml of 4201 culture medium was added to each experimental well in a 96-well plate. The cells were seeded in the plate and cultured at 37°C with 5% CO₂ until they had fully covered the bottom of each well; 150 ml of stimulant was added to each well, and each sample was repeated in 3 wells. The cells were then cultured at 37°C with 5% CO₂ and observed under an inverted microscope after 24, 48, and 72 h of culturing. MTT solution (20 ml; 5 mg/mL, or 0.5% MTT) was then added to each well, and the cells were cultured for another 4 h. The medium in each well was carefully removed, followed by the addition of 150 ml dimethyl sulfoxide and incubation on a shaker at low speed for 10 min to fully dissolve the crystalized precipitate. The absorbance of each well was measured at 490 nm using a microplate reader.

DCFH-DA flow cytometry to detect ROS production in cells: Cells in exponential growth phase were collected. After adjusting the cell density of the suspension, 5 mL of 4201 culture medium was added to each flask, and the density of the cells to be tested was adjusted to 5×10⁵/flask. The cells were cultured at 37°C with 5% CO₂ until they had adhered to the flask wall, and the culture medium was replaced with medium

Table 1. PCR primer sequences.

Primer	Sequence	Product size
β -actin	5'-CCATGTCAGTTGCTATCCAGG-3' 5'-TCTCCTTAATGTCACGCACGA-3'	252 bp
FN	5'-CCGCCATTAATGAGAGTGAT-3' 5'-AGTTAGTTGCGGCAGGAGAAG-3'	133 bp
TGF- β	5'-GCCCTGGACACCAACTATTGC-3' 5'-AGGCTCCAAATGTAGGGGCAGG-3'	161 bp

containing different stimulants. The cells were cultured at 37°C with 5% CO₂ for 24, 48, and 72 h, collected with 600 ml trypsin and counted; 20 000 cells/mL were centrifuged at 1000 rpm and 4°C for 5 min, and the supernatant was discarded. The cells were gently resuspended in 1 mL of 4201 culture medium containing 10 mmol/L DCFH-DA, followed by culturing in an incubator at 37°C for 30 min. The cells and probe were mixed thoroughly for 30 min by inverting the flask once every 3–5 min. The cell suspension was then centrifuged at 1000 rpm for 5 min at 4°C, and the supernatant was discarded. The cells were resuspended and washed 3 times with 1 mL serum-free medium to completely remove the DCFH-DA that did not enter the cells. The cells were then centrifuged again at 1000 rpm and 4°C for 5 min, and the supernatant was discarded, followed by the addition of 500 ml phosphate-buffered saline (PBS) to resuspend the cells. After 30 min, the cells were subjected to flow cytometry (using the parameters set for FITC) at an excitation wavelength of 488 nm and an emission wavelength at 525 nm to detect the fluorescence intensity before and after stimulation.

Western blotting was used to detect the activity of the PI3K/Akt/mTOR and TGF- β 1/Smad pathways and expression of TGF- β 1, FN, Smad2/3, Smad7 proteins: Cells were collected from each group, and 60 μ L protein lysis buffer and 0.6 μ L protease inhibitor were added, followed by ultrasonication for 20 min and centrifugation at 1200 \times g for 5 min. The supernatant was collected as the total protein sample, and the bicinchoninic acid (BCA) method was used to measure the protein concentration, which was then adjusted to 5 μ g/ μ L. The protein samples were separated by 7.5%, 10%, and 12% sodium dodecyl sulfate-polyacrylamide gel electrophoresis (SDS-PAGE) and then transferred to polyvinylidene fluoride (PVDF) membranes. The membranes were blocked with 5% skim milk powder or 3% bovine serum albumin (BSA) at room temperature for 2 h, followed by incubation with the primary antibody at 4°C overnight. The membrane was then washed with Tris-buffered saline-Tween 20 (TBST) and incubated with the secondary antibody at room temperature for 2 h. The membrane was washed again with TBST, followed by the addition of enhanced electrochemiluminescence (ECL) reagent and observation.

Real-time qPCR was performed to detect TGF- β 1 and FN mRNA expression: Total RNA was extracted from mesangial cells using TRIzol reagent (Invitrogen, US) according to the manufacturer's manual, and 4 μ g total RNA was taken from each sample to synthesize cDNA using random primers and Moloney murine leukemia virus (MMLV) reverse transcriptase. Real-time qPCR was performed using the Rotor-Gene 3000 PCR system. The primers were synthesized by TaKaRa (Dalian, China) (Table 1). In brief, 2 μ L cDNA was added to a 20- μ L reaction system (containing 2.5 μ L 2.5 nmol/ μ L deoxynucleotides (dNTPs), 10 μ L 10 \times SYBR Green I PCR buffer, 1.5 μ L 25 mmol/L MgCl₂, 1 μ L each of upstream and downstream primers, and 1 U Taq polymerase). The reaction proceeded at 94°C for 5 min for pre-denaturation, followed by 40 cycles of denaturation at 95°C for 10 s, annealing at 60°C for 30 s, and extension at 72°C for 30 s. β -Actin was used as the internal standard, and the experimental data were processed using the 2^{- $\Delta\Delta$ CT} method to calculate the mRNA/ β -actin mRNA ratio for each sample. The experiment was repeated 3 times for each experimental group.

Statistical analysis: All data were analyzed using SPSS17.0 software. The experimental data are expressed as the mean \pm standard deviation ($\bar{x}\pm s$). Univariate analysis of variance (ANOVA) was used for intergroup comparisons, and the least significant difference (LSD) method was employed for pairwise comparison. Differences were considered statistically significant at $p < 0.05$.

Results

Comparison of the mesangial cell proliferation rate in different groups

The proliferation rates of mesangial cells in each group were measured using an MTT assay after 24, 48, 72 h of culturing. Based on the results, the difference in the proliferation rate was most obvious in the 48-h group, and no statistically significant difference in proliferation rate was found for the hypertonic control group compared with the NG group ($p > 0.05$). The proliferation rate of cells in the HG group was significantly higher than that in the NG group ($p < 0.05$). Compared with

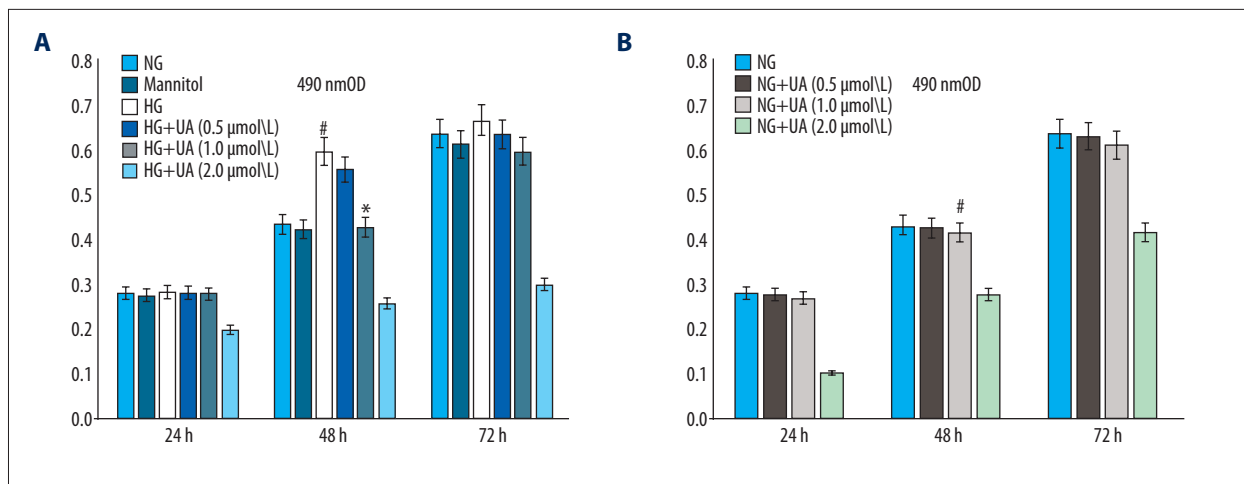


Figure 1. (A) UA inhibited the mesangial cell proliferation induced by high glucose (determined by an MTT assay). # $p < 0.01$ compared with the NG group; * $p < 0.05$ compared with the HG group. (B) UA (1.0 $\mu\text{mol/L}$) did not affect the mesangial cell growth induced by normal glucose. NG – normal glucose culture group; Mannitol – hypertonic control group; HG – high glucose culture group; UA – ursolic acid.

the HG group, mesangial cells exhibited a dose-dependent reduction in proliferation at 48 h after treatment with different concentrations of UA (0.5, 1.0, and 2.0 mmol/L ; Figure 1A). In contrast, the normal growth rate of mesangial cells was not affected after treatment with different concentrations of UA (0.5 and 1.0 $\mu\text{mol/L}$) in the NG group (Figure 1B).

Changes in ROS production in mesangial cells

A DCFH-DA probe was used to detect ROS levels in mesangial cells via flow cytometry, and the results revealed higher ROS production in cells of the HG group than in NG group cells ($p < 0.05$). HG+UA group (1.0 mmol/L) cells exhibited significantly decreased ROS production compared with the HG group ($p < 0.05$; Figure 2).

Changes in p-Akt/Akt and p-mTOR/mTOR protein expression

After 48 h of culturing, markedly higher levels of p-Akt (ser473) and p-mTOR (ser2448) ($p < 0.05$) proteins were observed in HG group mesangial cells than in cells of the NG group. UA (1.0 mmol/L) significantly inhibited HG-induced Akt and mTOR phosphorylation in mesangial cells (Figure 3).

Changes in mRNA and protein expression of TGF β 1 in mesangial cells detected by real-time PCR and Western blotting

The results of real-time PCR and Western blotting showed that TGF β 1 mRNA and protein expression in mesangial cells increased significantly ($p < 0.05$) in the HG group after 48 h of culturing. UA (1.0 mmol/L) significantly inhibited HG-induced

TGF β 1 mRNA and protein expression in mesangial cells ($p < 0.05$; Figure 4).

Changes in FN mRNA and protein expression detected by RT-PCR and Western blotting

Real-time PCR and immunoblotting revealed significantly increased FN mRNA and protein expression in HG group mesangial cells ($p < 0.05$) after 48 h of culturing. UA (1.0 mmol/L) significantly inhibited HG-induced FN mRNA and protein expression in mesangial cells ($p < 0.05$; Figure 5).

Changes in Smad2/3 and Samd7 protein expression detected by Western blotting

Immunoblotting revealed significantly increased Smad2/3 protein expression and significantly decreased Smad7 in HG group mesangial cells ($p < 0.05$) after 48 h of culturing. UA (1.0 mmol/L) significantly inhibited HG-induced Smad2/3 protein expression in mesangial cells ($p < 0.05$). In contrast, UA (1.0 mmol/L) significantly promoted HG-induced Smad7 protein expression in mesangial cells ($p < 0.05$; Figure 6).

Discussion

PI3K/Akt/mTOR signaling is a classical pathway widely found in eukaryotic cells that regulates a variety of cellular functions, such as glucose metabolism, glycogen synthesis, protein synthesis, cell proliferation, cell hypertrophy, and cell death [4]. In this study, we observed elevated p-Akt and p-mTOR expression in human mesangial cells exposed to HG stimulation for 48 h, along with activation of the PI3K/Akt/mTOR pathway, abnormal

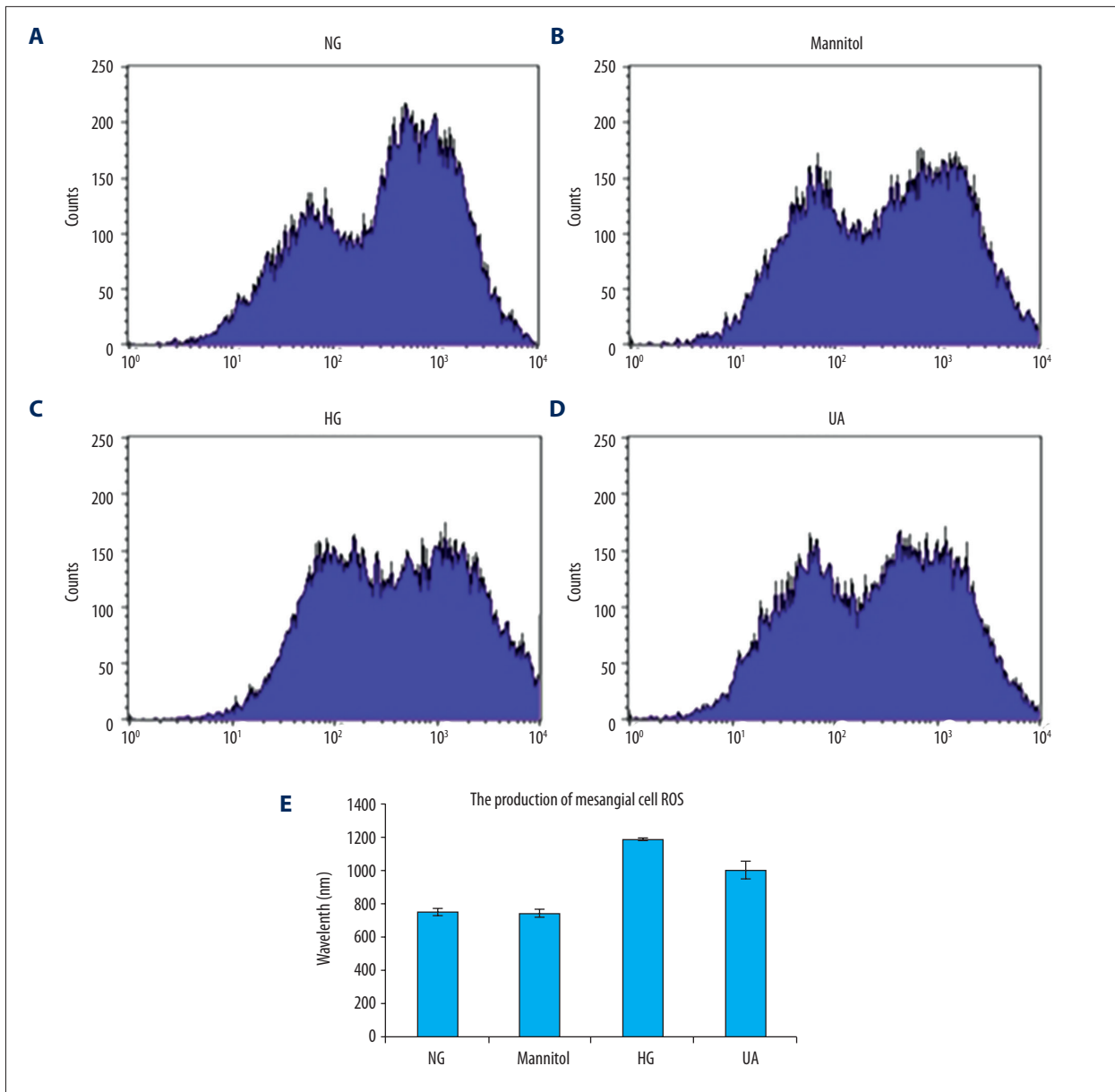


Figure 2. Ursolic acid (UA) significantly inhibited the ROS production in mesangial cells induced by high glucose levels. **(A)** NG, normal glucose group (5 mmol/L glucose); **(B)** Mannitol, hypertonic control group (5 mmol/L glucose+24.5 mmol/L mannitol); **(C)** HG, high glucose group (30 mmol/L glucose); **(D)** UA, UA treatment group (30 mmol/L glucose+1.0 mmol/L UA); **(E)** semi-quantitative analysis. # p<0.01 compared with the NG group; * p<0.05 compared with the HG group.

proliferation, and overexpression of the cytokine TGFβ1 and ECM protein FN, suggesting that PI3K/Akt/mTOR signaling is involved in HG-mediated mesangial cell damage. Consistent with our results, the *in vitro* study by Chen et al. [13] also demonstrated that HG activated the PI3K/Akt signaling pathway, downregulated downstream FoxO3α expression, promoted oxidative stress, and enhanced ECM deposition, suggesting that this pathway may be involved in the pathogenesis of DN [14].

Oxidative stress refers to excessive production of ROS and reactive nitrogen species (RNS) in response to various harmful stimuli that exceeds the oxygen-scavenging capacity of the body and causes an imbalance between the oxidation and antioxidant systems, leading to tissue damage. In recent years, many studies have suggested that stimulation by a variety of factors, such as HG, the inflammatory response, mechanical traction, and lipid deposition, induces oxidative stress in glomerular mesangial cells and promotes the development and progression of glomerulosclerosis [15,16]. Moreover,

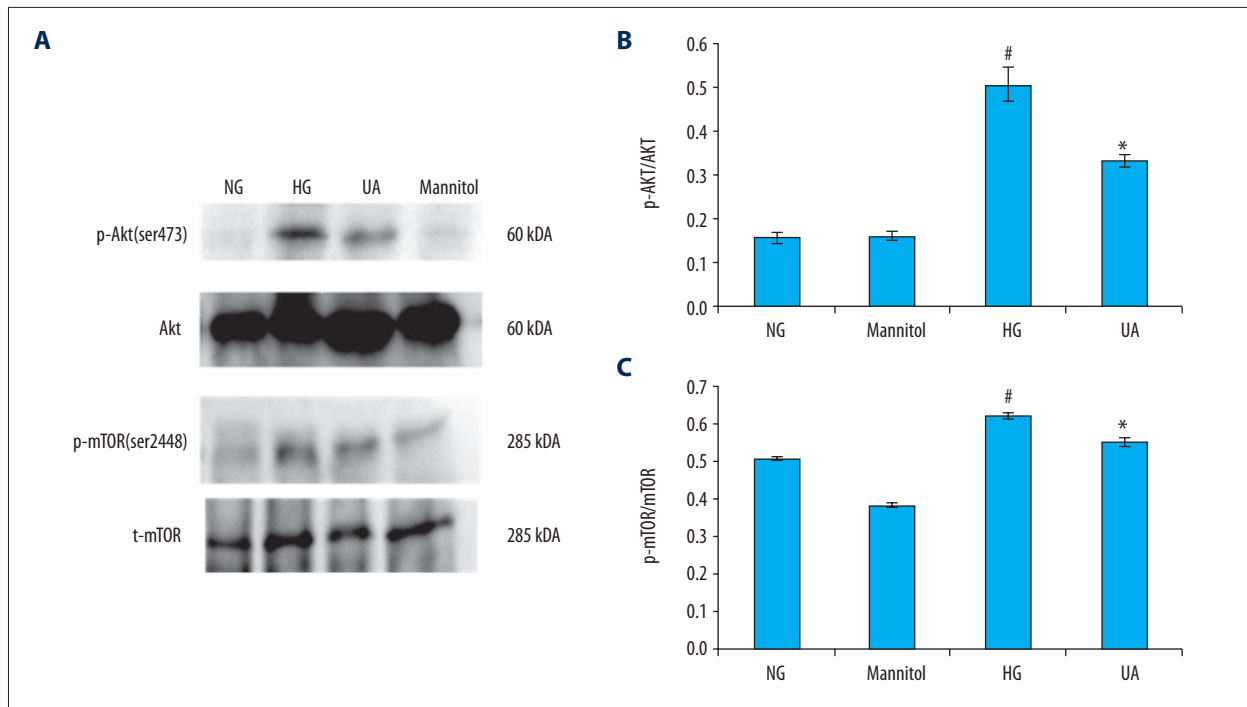


Figure 3. (A–C) Western blotting was used to detect PI3K/Akt/mTOR pathway activity in mesangial cells of each group. NG: normal glucose group (5 mmol/L glucose); Mannitol: hypertonic control group (5 mmol/L glucose+24.5 mmol/L mannitol); HG: high glucose group (30 mmol/L glucose); HG+UA: ursolic acid treatment group (30 mmol/L glucose+1.0 mmol/L ursolic acid). # $p < 0.05$ compared with the NG group; * $p < 0.05$ compared with the HG group.

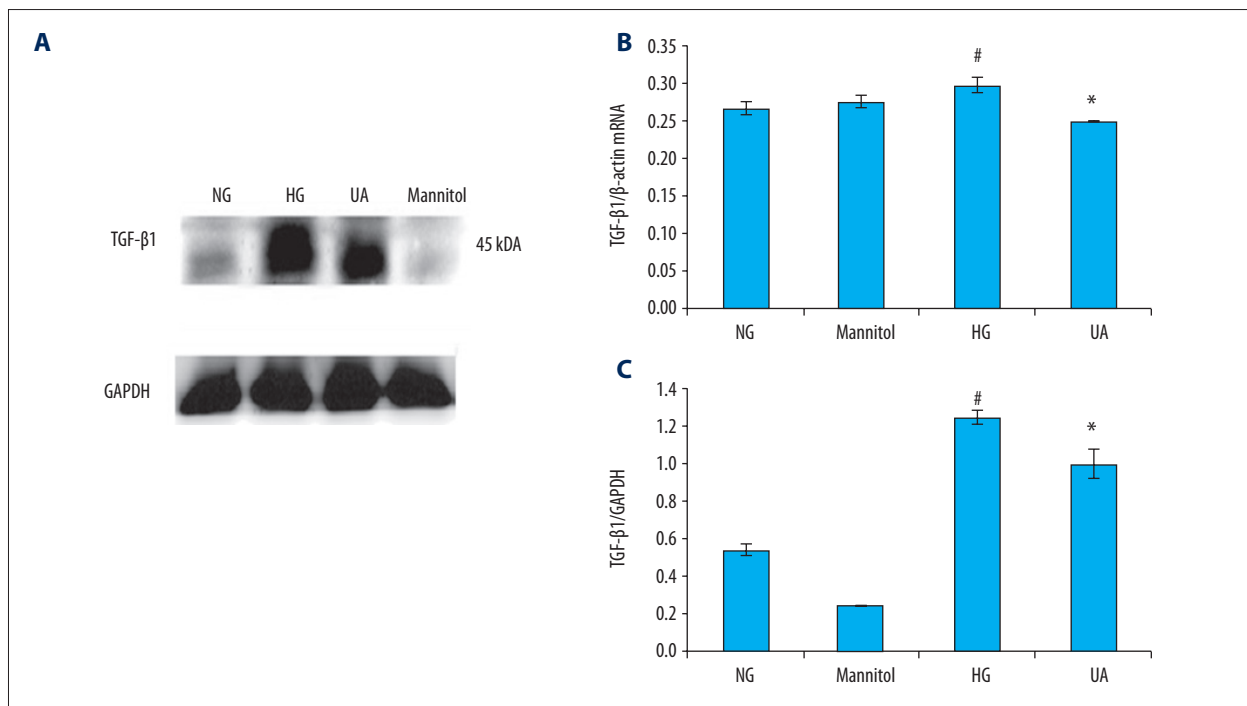


Figure 4. (A–C) mRNA and protein expression of TGFβ1 in mesangial cells detected by RT-PCR and Western blotting. NG: normal glucose group (5 mmol/L glucose); Mannitol: hypertonic control group (5 mmol/L glucose+24.5 mmol/L mannitol); HG: high glucose group (30 mmol/L glucose); HG+UA: ursolic acid treatment group (30 mmol/L glucose+1.0 mmol/L ursolic acid). # $p < 0.05$ compared with the NG group; * $p < 0.05$ compared with the HG group.

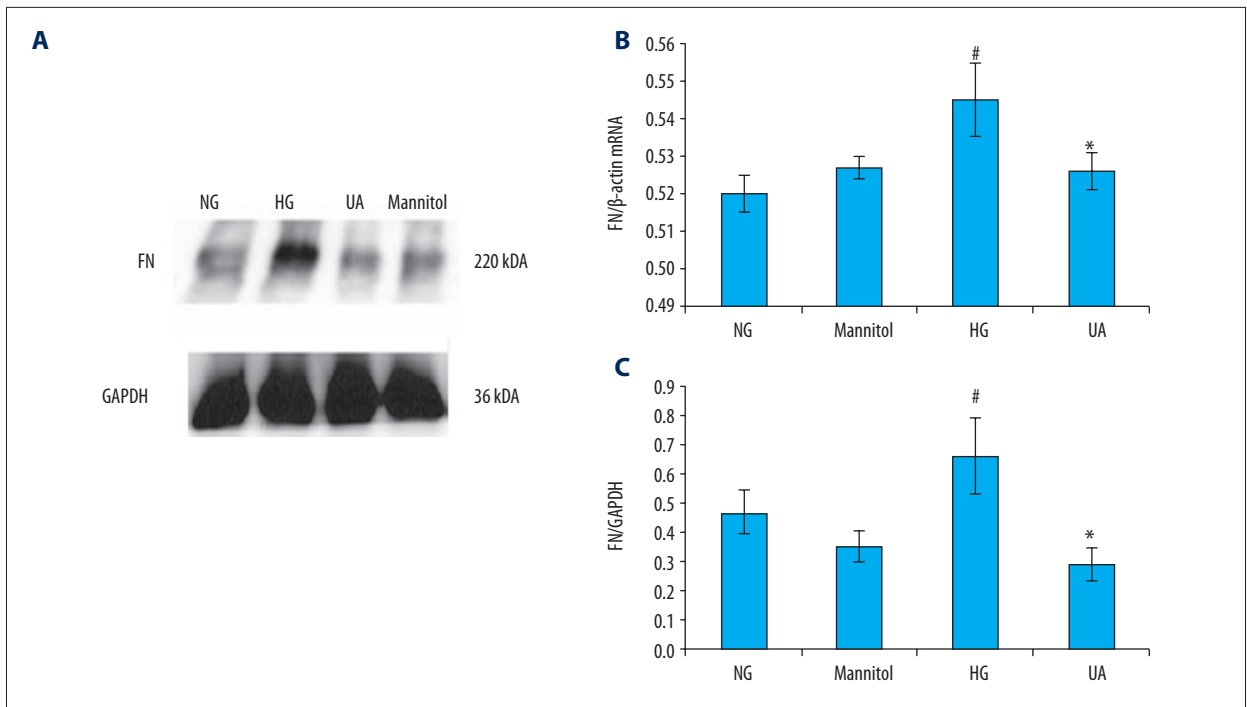


Figure 5. (A–C) FN mRNA and protein expression in mesangial cells detected by real-time PCR and Western blotting. NG: normal glucose group (5 mmol/L glucose); Mannitol: hypertonic control group (5 mmol/L glucose+24.5 mmol/L mannitol); HG: high glucose group (30 mmol/L glucose); HG+UA: ursolic acid treatment group (30 mmol/L glucose+1.0 mmol/L ursolic acid). # p<0.05 compared with the NG group; * p<0.05 compared with the HG group.

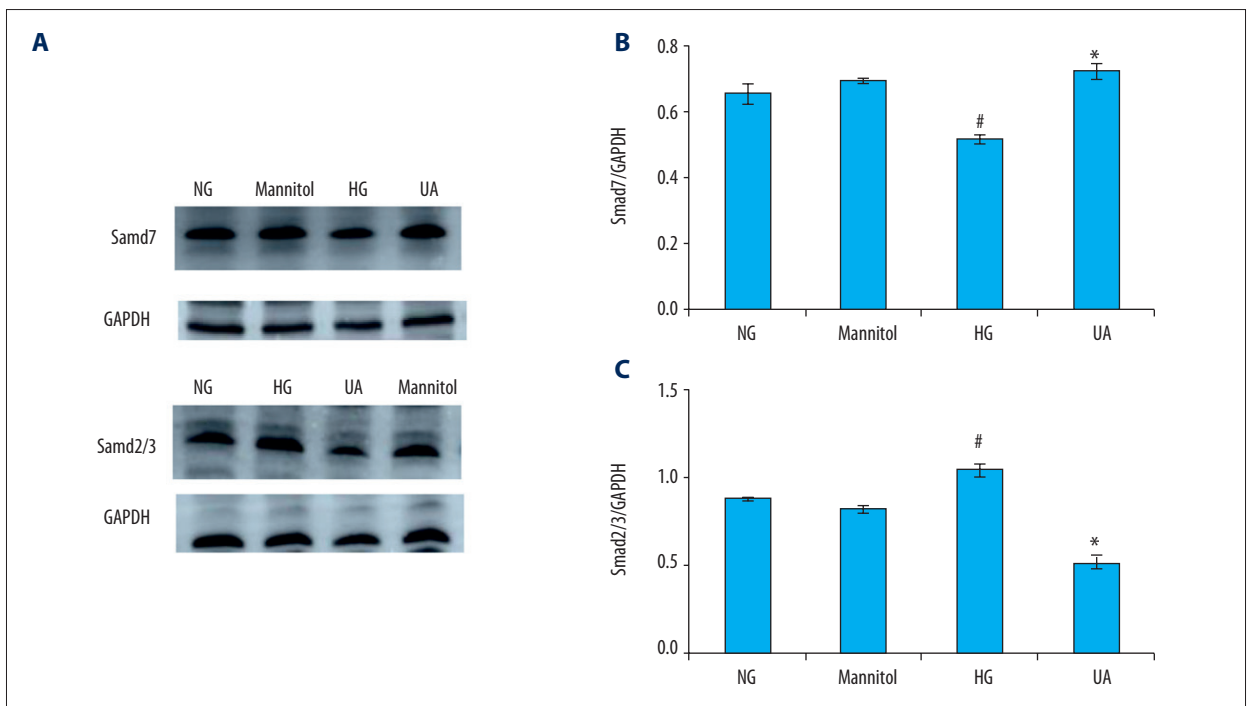


Figure 6. (A–C) Smad2/3 and Smad7 protein expression detected by Western blotting. NG: normal glucose group (5 mmol/L glucose); Mannitol: hypertonic control group (5 mmol/L glucose+24.5 mmol/L mannitol); HG: high glucose group (30 mmol/L glucose); HG+UA: ursolic acid treatment group (30 mmol/L glucose+1.0 mmol/L ursolic acid). # p<0.05 compared with the NG group; * p<0.05 compared with the HG group.

overproduction of ROS, which are important intracellular signaling messengers that activate multiple signal transduction pathways, can indirectly lead to tissue and cell damage. In this study, we found that HG increased ROS production and oxidative stress, induced excessive TGF β 1 secretion, and enhanced FN expression in mesangial cells. Similarly, Jeong et al. revealed that HG activates the PI3K/Akt-ERK1/2 and p38 MAPK pathways, promotes ROS production, and enhances the activity of NADPH oxidase, resulting in ECM accumulation [17]. In this study, we found that HG increased Samd2/3 production and decreased Samd7 production, inducing excessive TGF β 1 secretion. Barnes et al. also found that ROS induce excessive TGF β 1 secretion from mesangial cells by activating the angiotensin II-TGF β 1-Smad pathway, promoting ECM deposition, and reducing ECM degradation [18,19].

UA is a plant-derived pentacyclic triterpene that is widely found in berries, fruits, and herbs. UA has anti-tumor, anti-liver fibrosis, hypoglycemic, hypolipidemic, and anti-atherosclerotic effects [6–11], and previous studies have found that this triterpene inhibits proliferation of cultured Jurkat cells (malignant tumor cells) and induces their apoptosis by suppressing PI3K/Akt pathway activation [20]. Thus, UA is expected to become a new treatment for hematological malignancies. Furthermore, UA inhibits proliferation and induces apoptosis of human hepatic stellate cells by reducing TGF- β mRNA expression, thereby mitigating the vicious cycle of hepatic fibrosis. UA and its homolog oleanolic acid decrease levels of fasting blood glucose, glycosylated hemoglobin, and urinary albumin in diabetic mice in a dose-dependent manner, possibly by increasing blood insulin levels and suppressing renal aldose reductase

(AR) activation. In addition, UA regulates transcription of phosphoenolpyruvate carboxykinase (PEPCK) and phosphorylation of its downstream effector insulin receptor substrate-2 (IRS-2) by enhancing expression of the PPAR α protein in liver tissues; this affects cytokine and free fatty acid (FFA) levels in serum, as well as TNF- α and adiponectin levels, thereby improving insulin resistance and lowering blood lipid levels in KKAY mice. UA was also found to inhibit mononuclear cell aggregation in blood and atherosclerosis in a dose-dependent manner in low-density lipoprotein (LDL) receptor-deficient mice induced by streptozotocin, likely by inhibiting the diabetes-induced pro-inflammatory response. However, the protective effect of UA in DN and the associated mechanism have not yet been fully clarified; therefore, further studies are needed.

Conclusions

In this study, we found that UA inhibited the mesangial cell proliferation induced by HG in a dose-dependent manner, suppressed expression of the cytokine TGF- β 1, and reduced FN expression and ECM deposition. Aside from the TGF- β 1/Samd signaling pathway, the protective effect of UA is also likely achieved through inhibition of PI3K/Akt/mTOR pathway activation. Furthermore, UA contains a hydroxyl group in its C₃ side chain that has antioxidant activity, thereby allowing UA to inhibit ROS production. The findings of this study further our understanding of the pharmacological effects of UA and provide new strategies and methods for treatment of DN using Chinese herbal medicines.

References:

1. El-Haddad B, Reule S, Drawz PE: Dual renin-angiotensin-aldosterone system inhibition for the treatment of diabetic kidney disease: Adverse effects and unfulfilled promise. *Curr Diab Rep*, 2015; 15(10): 70
2. Slyne J, Slattery C, McMorrow T, Ryan MP: New developments concerning the proximal tubule in diabetic nephropathy: *In vitro* models and mechanisms. *Nephrol Dial Transplant*, 2015; 30(4): 60–67
3. Uttarwar L, Gao B, Ingram AJ, Krepinsky JC: SREBP-1 activation by glucose mediates TGF-beta upregulation in mesangial cells. *Am J Physiol Renal Physiol*, 2012; 302(3): F329–41
4. Luna-Acosta JL, Alba-Betancourt C, Martínez-Moreno CG et al: Direct anti-apoptotic effects of growth hormone are mediated by PI3K/Akt pathway in the chicken bursa of Fabricius. *Gen Comp Endocrinol*, 2015; 224: 148–59
5. Wang C, Liu X, Ke Z et al: Mesangial medium from IgA nephropathy patients induces podocyte epithelial-to-mesenchymal transition through activation of the phosphatidylinositol-3-kinase/Akt signaling pathway. *Cell Physiol Biochem*, 2012; 29(5–6): 743–52
6. Jamal M, Imam SS, Aqil M et al: Transdermal potential and anti-arthritis efficacy of ursolic acid from niosomal gel systems. *Int Immunopharmacol*, 2015; 29(2): 361–69
7. Sundaresan A, Radhiga T, Pugalendi KV: Effect of ursolic acid and Rosiglitazone combination on hepatic lipid accumulation in high fat diet-fed C57BL/6J mice. *Eur J Pharmacol*, 2014; 741: 297–303
8. Lee J, Lee HI, Seo KI et al: Effects of ursolic acid on glucose metabolism, the polyol pathway and dyslipidemia in non-obese type 2 diabetic mice. *Indian J Exp Biol*, 2014; 52(7): 683–91
9. Castro AJ, Frederico MJ, Cazarolli LH et al: The mechanism of action of ursolic acid as insulin secretagogue and insulinomimetic is mediated by cross-talk between calcium and kinases to regulate glucose balance. *Biochim Biophys Acta*, 2015; 1850(1): 51–61
10. Jyoti MA, Zerín T, Kim TH et al: *In vitro* effect of ursolic acid on the inhibition of *Mycobacterium tuberculosis* and its cell wall mycolic acid. *Pulm Pharmacol Ther*, 2015; 33: 17–24
11. Nelson AT, Camelio AM, Claussen KR et al: Synthesis of oxygenated oleanolic and ursolic acid derivatives with anti-inflammatory properties. *Bioorg Med Chem Lett*, 2015; 25(19): 4342–46
12. Zhang T, Su J, Guo Bet al: Ursolic acid alleviates early brain injury after experimental subarachnoid hemorrhage by suppressing TLR4-mediated inflammatory pathway. *Int Immunopharmacol*, 2014; 23(2): 585–91
13. Chen G, Wang T, Uttarwar L et al: SREBP-1 is a novel mediator of TGF β 1 signaling in mesangial cells. *J Mol Cell Biol*, 2014; 6(6): 516–30
14. Zhang L, Pang S, Deng B et al: High glucose induces renal mesangial cell proliferation and fibronectin expression through JNK/NF-kappaB/NADPH oxidase/ROS pathway, which is inhibited by resveratrol. *Int J Biochem Cell Biol*, 2012; 44(4): 629–38
15. Jeong SI, Kim SJ, Kwon TH et al: Schizandrin prevents damage of murine mesangial cells via blocking NADPH oxidase-induced ROS signaling in high glucose. *Food Chem Toxicol*, 2012; 50(3–4): 1045–53
16. Teles F, da Silva TM, da Cruz Júnior FP et al: Brazilian red propolis attenuates hypertension and renal damage in 5/6 renal ablation model. *PLoS One*, 2015; 10(1): e0116535

17. Wang Y, Wang Y, Liu D et al: Cordyceps sinensis polysaccharide inhibits PDGF-BB-induced inflammation and ROS production in human mesangial cells. *Carbohydr Polym*, 2015; 125: 135–45
18. Alique M, Sánchez-López E, Rayego-Mateos S et al: Angiotensin II, via angiotensin receptor type 1/nuclear factor- κ B activation, causes a synergistic effect on interleukin-1- β -induced inflammatory responses in cultured mesangial cells. *J Renin Angiotensin Aldosterone Syst*, 2015; 16(1): 23–32
19. Ding K, Wang Y, Jiang W et al: Qian Yang Yu Yin Granule-containing serum inhibits angiotensin II-induced proliferation, reactive oxygen species production, and inflammation in human mesangial cells via an NADPH oxidase 4-dependent pathway. *BMC Complement Altern Med*, 2015; 15: 81
20. Ou X, Liu M, Luo H et al: Ursolic acid inhibits leucine-stimulated mTORC1 signaling by suppressing mTOR localization to lysosome. *PLoS One*, 2014; 9(4): e95395